A numerical study on the influence of insulating layer of the hot disk sensor on the thermal conductivity measuring accuracy

Hu Zhang, Yu Jin, Wei Gu, Zeng-Yao Li and Wen-Quan Tao*

Key Laboratory of Thermo-Fluid Science and Engineering, Ministry of Education,
Xi'an Jiaotong University,
Xi'an, 710049, China
Fax: 029-82669106
E-mail: huzhang522@stu.xjtu.edu.cn
E-mail: guwei.y@stu.xjtu.edu.cn
E-mail: jinyu618@stu.xjtu.edu.cn
E-mail: lizengy@mail.xjtu.edu.cn
E-mail: wqtao@mail.xjtu.edu.cn
*Corresponding author

Abstract: A numerical study on the influence of the insulation layer of the hot disk sensor on the thermal conductivity measuring accuracy has been conducted. It is found that the influences of the thermal contact resistance and the insulating layer could be excluded in the transient plane source method. Both the kapton5501 and the mica5082 sensor could measure stainless steel and ceramic with a deviation less than 3% while the deviation increases to 54.2% of silica aerogel because of the large heat loss proportion through the mica5082 sensor side. The simulation proved that the heat loss through sensor side and accuracy could be improved by increasing the radius of the sensor.

Keywords: numerical; insulation layer influence; thermal conductivity; accuracy; transient plane source; experiments.

Reference to this paper should be made as follows: Zhang, H., Jin, Y., Gu, W., Li, Z-Y. and Tao, W-Q. (2013) 'A numerical study on the influence of insulating layer of the hot disk sensor on the thermal conductivity measuring accuracy', *Progress in Computational Fluid Dynamics*, Vol. 13, Nos. 3/4, pp.195–205.

Biographical notes: Hu Zhang is currently a Doctoral candidate in the MOE Key Laboratory of Thermo-Fluid Science and Engineering at Xi'an Jiaotong University. His current research is mainly focused on the heat transfer mechanism in micro/nano scale porous materials and the apparent thermal conductivity measurement of super insulation material in complex environment.

Yu Jin is currently a Doctoral candidate in the MOE Key Laboratory of Thermo-Fluid Science and Engineering at Xi'an Jiaotong University. His current research is mainly focused on numerical simulation on fin-and-tube heat exchangers.

Wei Gu is currently a Doctoral candidate in the MOE Key Laboratory of Thermo-Fluid Science and Engineering at Xi'an Jiaotong University. His current research is mainly focused on the micro/nano scale radiation heat transfer.

Zeng-Yao Li is an Associate Professor in the MOE Key Laboratory of Thermo-Fluid Science and Engineering at Xi'an Jiaotong University. He received his PhD in 2002. His research field includes heat transfer enhancement, solar energy and micro/nano scale heat transfer of porous material.

Wen-Quan Tao is a Professor in the MOE Key Laboratory of Thermo-Fluid Science and Engineering at Xi'an Jiaotong University. His research interests include numerical heat transfer and its industrial applications, fluid flow and heat transfer in micro-channel, multiscale simulation of fluid flow and heat transfer problems, electronic package cooling technology and fuel cells.

This paper is a revised and expanded version of a paper entitled 'A numerical study on the influence of insulating layer of the hot disk sensor on the thermal conductivity measuring when using transient plane source method' presented at Third Asian Symposium on Computational Heat Transfer and Fluid Flow (ASCHT2011), Kyoto University, Japan, 22–26 September 2011.

1 Introduction

Thermal conductivity is one of the most important thermal properties. There are many ways of measuring thermal conductivity and it mainly divided into two categories, steady method and unsteady method. The unsteady method has advantages of fast, convenient and economic. Many studies have been conducted on the transient method. Transient hot wire, transient hot strip, laser flash and transient plane source are common transient thermal conductivity test methods (Gustafsson et al., 1979, 1986; Gustafsson, 1990; Xie et al., 2006; Hay et al., 2005; Saleh, and Al, 2006; Solorzano et al., 2008; Huang and Liu, 2009). Uncertainty analysis is an important issue of the transient method. Malinarič (2007) divided the sources of uncertainty in the dynamic test into two aspects. The first part represents uncertainties of input parameter measurements and the evaluation method and the other part comprises uncertainties caused by deviations of the mathematical model from the real experimental setup. Many works have been conducted for the first part. The theory of sensitivity coefficients has been adopted to analyse the time window for the experiment (Malinarič, 2007; Bohac et al., 2000; Suleiman and Malinarič, 2006). Malinarič and Suleiman (Malinarič, 2007; Suleiman and Malinarič, 2006, 2007; Suleiman, 2010) analysed the temperature measurement uncertainty on the parameter estimation using least-squares procedure and the data evaluation method to improve the performance of the transient plane source and dynamic plane source technique. The uncertainty of the measurement of voltage, resistance, diameter, thickness, temperature coefficient of the resistivity (TCR) of the sensor, etc., has been discussed by Suleiman and Malinarič (2007).

Among the transient methods, the transient plane source method has been used widely for its advantages of fast, non-destructive, large ranges ($0.01 < \lambda < 500$ W·m^{-1}·K^{-1}, 50 K < T < 1,000 K) and high accuracy (3%) as presented in ISO22007-2 (2008). The major purpose of the present paper is to analyse some uncertainty-related problems of the transient plane source method. The size of materials measured by hot wire, hot strip and transient plane source methods should be large enough to avoid the heat loss from outside of the test material otherwise it will failed to fit the infinite assumption of the measurement theory according to the standards of ISO (ISO22007-2, 2008; ISO8894-1, 1987; ISO8894-2, 2007; ISO22007-4, 2008). Due to the heat capacity of the heating element (nickel), the insulation layer, the binder (combines the nickel and the insulation layer) and the air gap (introduced by the surface roughness), there exists thermal resistance between the heating source and the surface of the test material facing the sensor. According to Gustafsson et al. (1979, 1986), Gustafsson (1990) and ISO22007-2 (2008), this kind of thermal resistance could be excluded in the measurement because these factors have effect on the thermal conductivity measurement at the very beginning of the whole measurement time in earlier studies. But how long the influence will last has never been indicated in the literature and it should be illustrated by some typical measurements for the convenience of users. The transient plane source method has an assumption that the heat source has no thickness and it is where the name plane source came from. However, the assumption is doubted when extremely low thermal conductivity material is measured by using mica insulating sensor because the heat loss through the sensor side may not be neglected. In addition, for a certain size material, how long it will take for the heat generated in the heating elements transfers to the outside of the test material is important for determining the measurement time. In the investigation of such problems numerical simulation may play an important role. For example, the influence of the finite dimensions of the actual samples in the hot wire technique has been studied (Cintra and dos Santos, 2000) with numerical simulation.

Although the detail measurement procedure of transient plane source method is already validated and established in the ISO 22007-2 standard, the validation of high insulation materials (like silica aerogels) at high temperature is not mentioned in the standard. The transient plane source method is recommended that polyimide, mcia, aluminium nitride or aluminium oxide be used as the insulation film, depending on the ultimate temperature of use. The hot disk thermal constants analyser conducts the measurement with the kapton sensor or mica sensor. The kapton sensor is used within the temperature ranges of 50 K–500 K because of the restrictions of kapton while the mica sensor is used at medium and higher temperature. The accuracy of kapton sensor is within ± 3% through validation with NIST1453 material (with thermal conductivity about 0.032 W·m^{-1}·K^{-1}) at room temperature in our work. The deviation between mica sensor and kapton sensor when measuring low thermal conductivity material such as silica aerogels is extremely large. Consequently, numerical simulation is adopted to analyse the reason of large deviation between mica sensor and kapton sensor when measuring low thermal conductivity material by reconsidering the assumptions of the transient plane source method.

In the present paper, the applicability of the assumption and the above questions for the transient plane source method are studied numerically. The simulation of the real heat transfer process of measuring stainless steel, ceramic and silica aerogel using different sensors of hot disk thermal constants analyser was conducted and the comparison was made to explain the experiment results. The accuracy of different sensors on measuring different materials was also discussed in this work. In the following, the theoretical basis of the measurement will first be briefly introduced for the reader's convenience, followed by the presentation of the adopted numerical methods. Then numerical results and discussion will be presented. Finally, some useful conclusions are summarised.

2 Theoretical basis

Transient plane source technology is proposed on the basis of transient hot wire method by Gustafsson (1990), and Gustafsson et al. (1979, 1986) and it became one of the ISO

standards (ISO22007-2, 2008) for the determination of thermal conductivity and thermal diffusivity simultaneously in 2008. The plane sensor consists of an electrically conducting element in the shape of double spiral, which has been etched out of a thin metal (nickel) foil. The spiral is sandwiched between two thin sheets of insulating material (kapton or mica) to keep the spiral shape and electric insulation. Figures 1(a) and 1(b) show the shapes of kapton5501 sensor and mica5082 sensor. When performing a thermal transport measurement, the sensor is fitted between two pieces of sample: each one with a plane surface facing the sensor as shown in Figure 1(c). The sensor is used both as a heat source and as a dynamic temperature sensor. In this article, simulation and experiment using kapton5501 sensor, mica5082 sensor, mica4921 sensor and mica4922 sensor were conducted. The kapton sensor covered by kapton insulation is designed for performing measurements bellow 500 K while mica sensor covered by mica insulation is designed for performing measurements at temperature as high as 1,000 K.

When the sensor is electrically heated, the resistance increases as a function of time and can be given by the following expression:

$$R(t) = R_0(1+\alpha\Delta T) = R_0\left[1+\alpha\Delta T_i + \alpha\Delta T(\tau)\right] \tag{1}$$

where t is the test time, s; R_0 is the resistance of the sensor at time t = 0, Ω; τ is the dimensionless time defined as $\tau = \sqrt{t/\Theta}$, here Θ is the characteristic time with form $\Theta = r^2/\alpha$, r is the radius of the sensor, mm, α is the thermal diffusivity of the test sample, $mm^2 \cdot s^{-1}$; α is the TCR, 1/K; ΔT is the mean temperature increase of the probe; ΔT_i is the temperature difference between the heat source and the sample surface facing the sensor, K; $\Delta T(\tau)$ is the temperature increase of the sample surface facing the sensor, K. The value of ΔT_i will becomes constant after a short time (it will be studied in this paper) provided the insulating layer is thin and the power output is constant. With the assumption that the bifilar probe can be approximated by a number of concentric and equally spaced circular line sources, the solution of the thermal conductivity equation is given by (Carslaw and Jaeger, 1986)

$$\Delta T(\tau) = \frac{P_0}{\pi^{3/2} r\lambda} D(\tau) \tag{2}$$

where P_0 is the power output of the sensor, W; λ is the thermal conductivity of the test sample, $W \cdot m^{-1} \cdot K^{-1}$; $D(\tau)$ is the dimensionless specific time function, defined as

$$D(\tau) = \left[m(m+1)\right]^{-2} \int_0^{\tau} \sigma^{-2} \left[\sum_{l=1}^{m} l \sum_{k=1}^{m} k \times \exp\left(\frac{-(l^2+k^2)}{4m^2\sigma^2}\right) I_0\left(\frac{lk}{2m^2\sigma^2}\right)\right] d\sigma \tag{3}$$

in which, I_0 is the modified Bessel function; m is the number of concentric ring sources.

Substituting equation (2) into equation (1) and denoting $R^* = R_0(1 + \alpha\Delta T_i)$, $C = \alpha R_0 P_0 / \pi^{3/2} r\lambda$, equation (1) can be rewritten as

$$R(t) = R^* + CD(\tau) \tag{4}$$

Figure 1 Sensor shape and test sample arrangement, (a) kapton5501 sensor (b) mica5082 sensor (c) sandwich structure (see online version for colours)

(a)

(b)

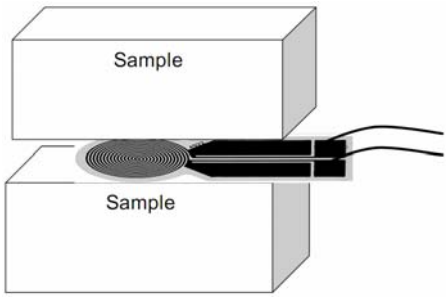

(c)

As discussed above, ΔT_i becomes constant after a short time and hence R^* has the same variation trend. C is a constant for an established measurement system. As shown in equation (4), $R(t)$ increases linearly with $D(\tau)$. When conducting the measurement, the input power and the heating time are given. The temperatures of the source (nickel) will increases when the probe begins to heat. The thermal resistance of the probe changes with temperature. The temperature increase of the source is obtained by measuring the voltage imbalance and the current according

to the test electrical bridge in the ISO standard. The temperature coefficient of resistance of the source is available. Then the temperature increase curve with time of the probe will be obtained. Finally, the linear relationship shown in equation (4) is established by a least-squares fitting procedure with the constraint condition of best linearity. Then the thermal diffusivity is obtained from the final step of the iteration procedure and the thermal conductivity is determined from the slop of the line.

3 Numerical simulation method

3.1 Computation domain

The problem at hand can be regarded as a transient heat conduction problem consisted of a series of very thin concentric heating elements in an infinite-large space. According to the axis-symmetrical geometry, the 3D heat conduction problem can be simplified into 2D one with one radian being adopted as the representative for the circumferential direction. A schematic diagram of the computational domain is shown in Figure 2. In the domain, zone 1 is the heat source (nickel), zone 2 is the insulation material (kapton or mica) and zone 3 is the test material.

The details of the geometry of the simulation conditions are presented in Table 1. Table 2 shows the thermal property used in the simulation. The simulation parameters of different materials are presented in Table 3.

Table 1 Simulation conditions

Sensor information	*Size*
Thickness and radius of test sample	15 mm/20 mm (25 for mica4921 and mica4922)
Thickness of nickel	7 μm
Thickness of kapton/mica	25 μm/115 μm
Space/width of nickel of kapton5501	0.3 mm/0.3 mm
Space/width of nickel of mica5082	0.2 mm/0.2 mm
Space/width of nickel of mica4921 and mica4922	0.5 mm/0.5 mm
Number of concentric ring sources of kapton5501 /mica5082/mica4921/mica4922	15/10/10/15
Radius of kapton5501/mica5082/ mica4921/mica4922	6 mm/6 mm/9.75 mm /14.75 mm

Table 2 Thermal property

Material	$\lambda/W{\cdot}m^{-1}{\cdot}K^{-1}$	$\rho/kg{\cdot}m^{-3}$	$cp/J{\cdot}kg^{-1}{\cdot}K^{-1}$
Nickel	91.4	8,900	444
Kapton	0.5	1,420	1100
Mica	0.75	1,600	880
Stainless steel	13.55	8,000	460
Ceramic	1.45	2,300	657
Silica aerogel	0.032	400	650

Table 3 Simulation parameters

Material	*Power/W*	*Iterative time step/s*	*Test time/s*	*Sensor*
Stainless steel	1	0.01	10	kapton5501/ mica5082
Ceramic	0.5	0.02	40	kapton5501/ mica5082
Silica aerogel	0.005	0.1	200	kapton5501/ mica5082
	0.01	0.1	200	mica4921
	0.02	0.1	200	mica4922

Figure 2 Schematic diagram of computation domain (see online version for colours)

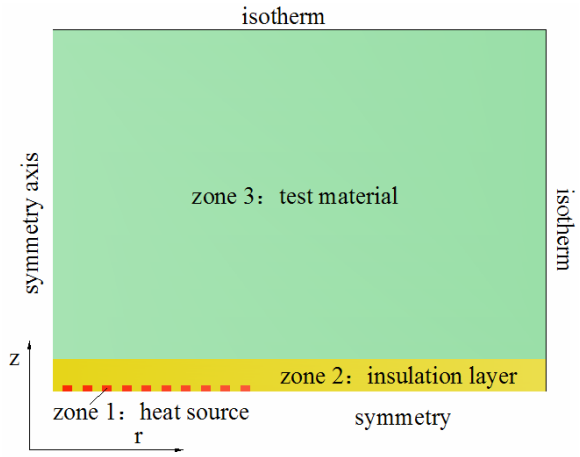

3.2 Governing equations and boundary conditions

The governing equations for the 2D axis-symmetrical cylindrical non-steady state heat conduction with an internal heat source can be expressed as follows:

$$\rho c\frac{\partial T}{\partial \tau}=\frac{1}{r}\frac{\partial}{\partial r}\left(\lambda r\frac{\partial T}{\partial r}\right)+\frac{\partial}{\partial z}\left(\lambda\frac{\partial T}{\partial z}\right)+\dot{\Phi} \tag{5}$$

The boundary conditions of the problem are shown as follows:

- Left side: axis symmetry.
- Downside: symmetry.
- Top of the test materials: $T = const$ (It is assumed that the propagation of the thermal disturbance in the heating elements has not reach the top surface yet).
- Right side: isothermal (the same assumption as for the top).
- Heat source: given different volumetric intensity of power input for different materials.
- Interfacial boundary: interior (It is a default boundary condition in FLUENT software. The continuity of temperature and heat flow on the interfacial boundary will be satisfied by the interior condition.)

3.3 Numerical methods

The simulation was conducted by commercial software FLUENT 6.3.26. The grid size was non-uniform because the geometry size of the heat source (μm), the insulating layer (μm) and the sample (mm) in the computational domain has different order of magnitude. The total grid number of different sensor was different. The grid numbers of kapton5501, mica5082, mica4921 and mica4922 are 1,026,000, 1,068,000, 1,286,250, and 1,755,400, respectively, with the cross section of each micro heating element can be distinguished individually. These grid numbers were obtained after the grid-independent examination. The 1st-order implicit formulation is adopted to solve the 2D unsteady state heat conduction problem, and the diffusion term is discretised by the central difference. The initial temperature of the computation domain is 300 K. The heat sources are treated as discrete heat sources with a finite volume. The temperatures of heat sources and the temperatures of sample surface facing insulation layer are non-uniform. The temperature of heat sources is obtained by volume average. The temperature of sample surface facing insulation layer is obtained by area weighted average.

4 Results and discussion

The idea of the simulation study is as follows: The thermal properties of different materials were given when conducting the numerical simulation. Then the temperature increase curves of the kapton and mica sensors were obtained through simulation. The temperature increase curve of the sensor was used to calculate the thermal conductivity and thermal diffusivity of the material based on the transient plane source method. Finally, comparisons of thermal properties between the computationally predicted values and given values are made to analyse the accuracy of kapton sensor and mica sensor without insulation layers. Following section provides the implementation details for sensor with insulation layer.

For the assessment of the sensor insulating layer influence on the thermal conductivity measuring accuracy following steps were conducted. First, the thermal conductivity and thermal diffusivity for different materials were measured by the hot disk thermal constants analysers. Since the temperature increase curve of the heating sensor obtained through simulation could not be used by the in-chip software supplied by the instrument. Programmes should be developed to calculate the thermal conductivity and thermal diffusivity from the temperature increase curve of the sensor obtained by numerical simulation. Then the simulation of kapton sensor and mica sensor without insulation layer was made to prove both kapton sensor and mica sensor could measure the thermal conductivity of different materials accurately when the assumption of plane source is fulfilled. Finally, the simulation of kapton sensor and mica sensor with real insulation layer was made and the simulation results were adopted to analyse the deviation between simulated and experimental data for mica sensor.

4.1 The validation of the thermal conductivity determination programmes

The programme developed in this paper for determining thermal conductivity and thermal diffusivity was validated by comparing with the experimental result conducted by the present authors using hot disk thermal constants analyser. Figure 3 shows the experiment result of temperature increases of the kapton5501 sensor and the mica5082 sensor at room temperature. The thermal conductivity and the thermal diffusivity of the test materials were obtained from such curves based on the theory of the transient plane source method briefly presented above. The programmes developed in this paper were to determine the thermal conductivity and thermal diffusivity of the materials once obtained the temperature increases of the test sensor and the test parameters (heating power, heating time and the geometric parameter of the sensor) from the simulation.

Figure 3 Temperature increases of silica aerogel of different sensors, (a) measured by kapton5501 and (b) measured by mica5082 (see online version for colours)

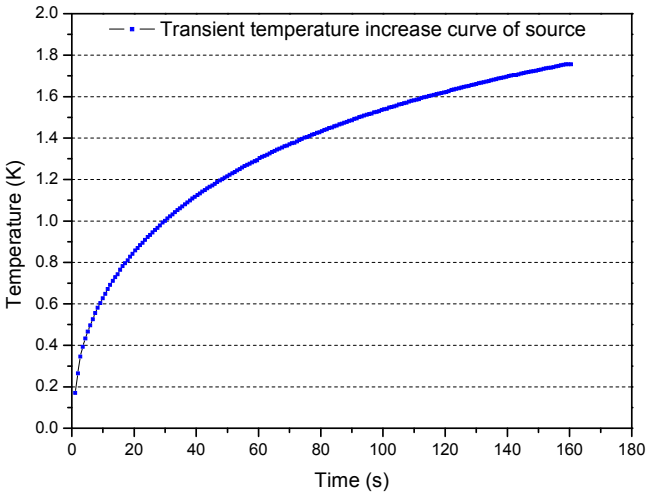

(a)

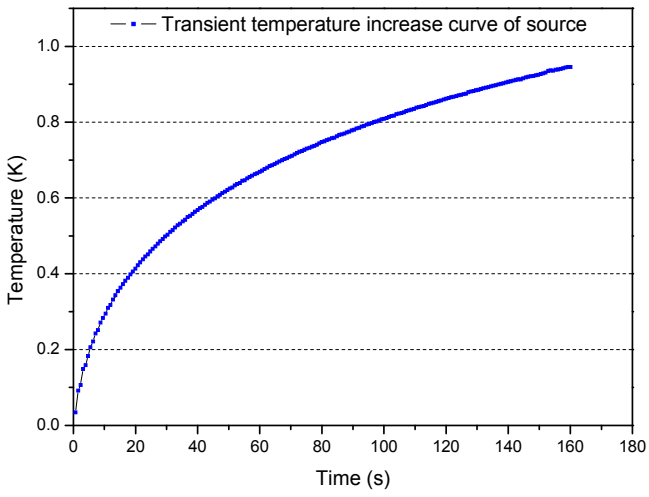

(b)

Table 4 Thermal conductivity and thermal diffusivity of silica aerogel

Thermal property	*kapton5501*		*mica5082*	
	$\lambda/W{\cdot}m^{-1}{\cdot}K^{-1}$	$\alpha/mm^2{\cdot}s^{-1}$	$\lambda/W{\cdot}m^{-1}{\cdot}K^{-1}$	$\alpha/mm^2{\cdot}s^{-1}$
Measured by hot disk	0.03504	0.1266	0.05403	0.1044
Calculated by programmes	0.03429	0.1245	0.05359	0.1062
Deviation/%	–2.14	–1.66	–0.81	1.72

Table 5 Comparisons of the given values and the computational values

Material	*Sensor*	$\lambda/W{\cdot}m^{-1}{\cdot}K^{-1}$			$\alpha/mm^2{\cdot}s^{-1}$		
		Given value	*Computational value*	*Deviation/%*	*Given value*	*Computational value*	*Deviation/%*
Silica aerogel	kapton5501	0.032	0.03146	–1.69	0.1231	0.1230	–0.06
	mica5082		0.03130	–1.85		0.1254	1.89
Stainless steel	kapton5501	13.55	13.30	–2.19	3.6821	3.6483	–0.92
	mica5082		13.17	–2.80		3.6463	–0.97

The thermal conductivity of silica aerogel was measured by the hot disk thermal constants analyser and the temperature increase curve was also calculated by the programmes as shown in Table 4. The accuracy of kapton5501 sensor was calibrated by NIST1453 at room temperature in this work and the accuracy was within ± 3%. For silica aerogel, the difference of the thermal property measured by kapton5501 sensor and mica5082 sensor were extremely large and the reason will be discussed in Section 4.2. The thermal conductivity and thermal diffusivity calculated by the programmes were close to the values obtained by the hot disk thermal constants analyser with maximum deviation –2.14%. The comparison proves that the programme developed in this paper is reliable and accurate on calculating the thermal conductivity and thermal diffusivity once obtained the sensor temperature increases with time.

4.2 The validation of the numerical simulation method with the thickness-negligible assumption

The transient plane source method assumes that the thickness of the sensor can be neglected. In this part, the numerical simulation method was validated with the assumption. Both the kapton5501 sensor and the mica5082 sensor are assumed without thickness when conducting the simulation. The temperature increases of silica aerogel and stainless steel with kapton5501 sensor and mica5082 sensor were obtained through the simulation. Then the thermal conductivity and thermal diffusivity were calculated by the programmes developed in Section 4.1.

The comparisons of the thermal conductivity and thermal diffusivity between the given values (setting in the simulation) and the computational values through the simulation were shown in Table 5. The comparison shows that when the sensor has no thickness, both the kapton5501 sensor and the mica5082 sensor could measure silica aerogel and stainless steel accurately with deviation less than ± 3%. The result demonstrates that the developed numerical simulation method could be adopted to analyse the test accuracy.

4.3 The time window affecting by the thermal resistance of the sensor insulation layer

As mentioned above, the temperature difference ΔT_i between the heat source and the surface of the sample facing the sensor becomes constant after a short time. Figures 4 to 6 show the average temperatures increase curve of source and sensor surface versus time for kapton5501 sensor and mica5082 sensor of the three materials: stainless steel, ceramic and silica aerogel, respectively. The temperature difference increases significantly with the increases of the thermal conductivity because the thermal resistance of the insulation layer takes up much larger proportion in the total thermal resistance when measuring larger thermal conductivity material. For stainless steel and ceramic, the temperature difference of mica sensor was larger than that of kapton sensor. For silica aerogel, the temperature difference was only several mK due to its extremely low thermal conductivity. The time periods required for temperature difference of different materials on different sensors to reach constant are shown in Table 6. The results show that the influence of thermal resistance of the sensor insulation layer will last less than 100 ms which is in good consistency with the value mentioned in ISO 22007-2.

Table 6 Time required for temperature difference to reach constant

Material	*mica5082/s*	*kapton5501/s*
Stainless steel	0.07	0.03
Ceramic	0.08	0.04
Silica aerogel	0.08	0.09

Figure 4 Temperature difference of stainless steel, (a) temperature increase and (b) temperature difference (see online version for colours)

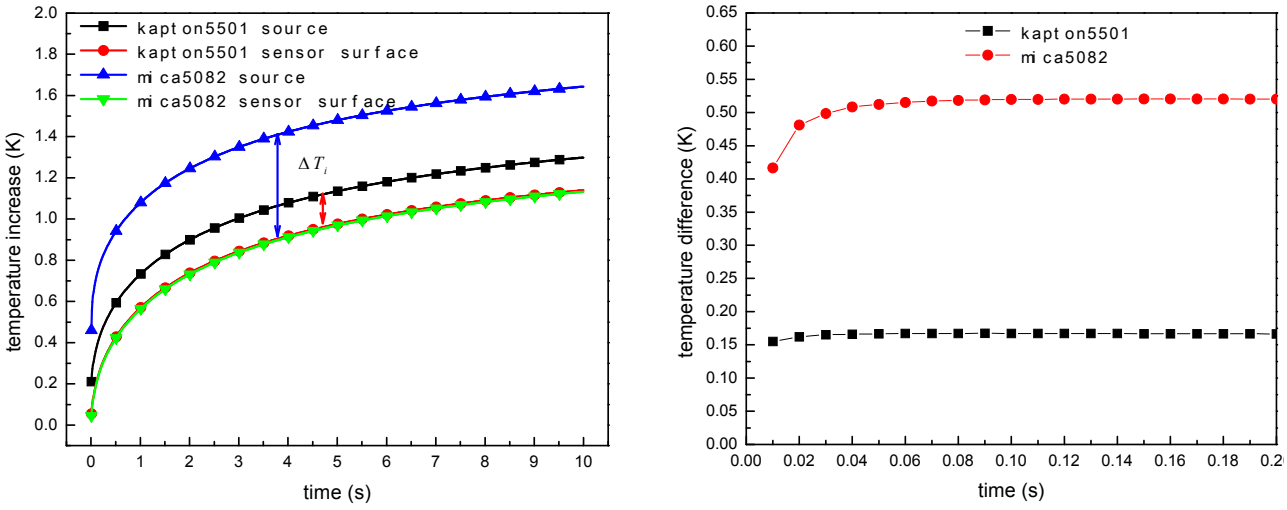

(a) (b)

Figure 5 Temperature difference of ceramic, (a) temperature increase and (b) temperature difference (see online version for colours)

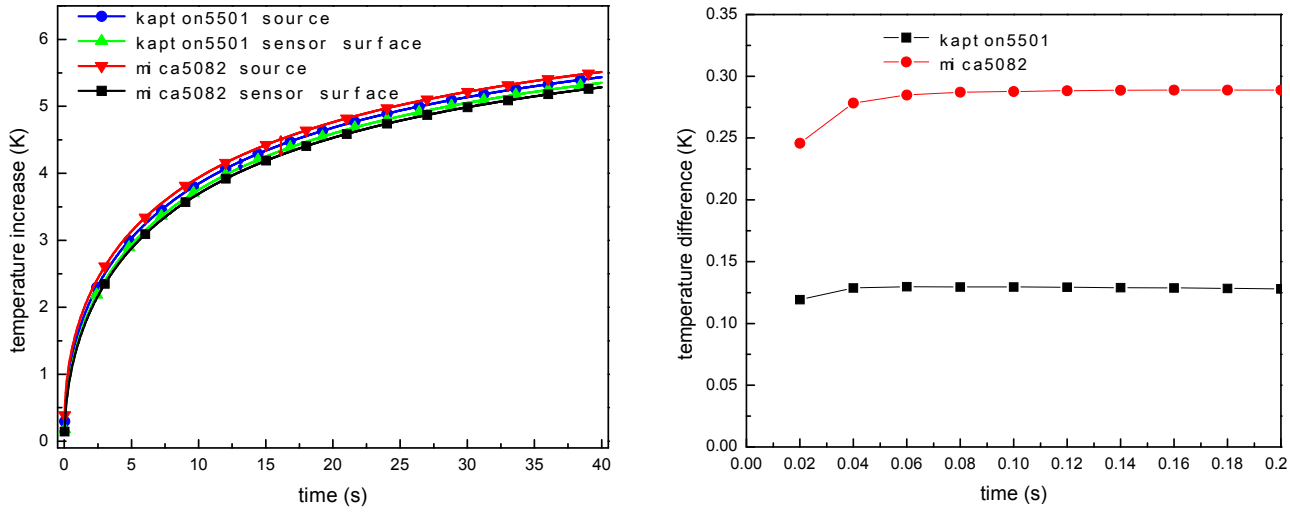

(a) (b)

Figure 6 Temperature difference of silica aerogel, (a) temperature increase and (b) temperature difference (see online version for colours)

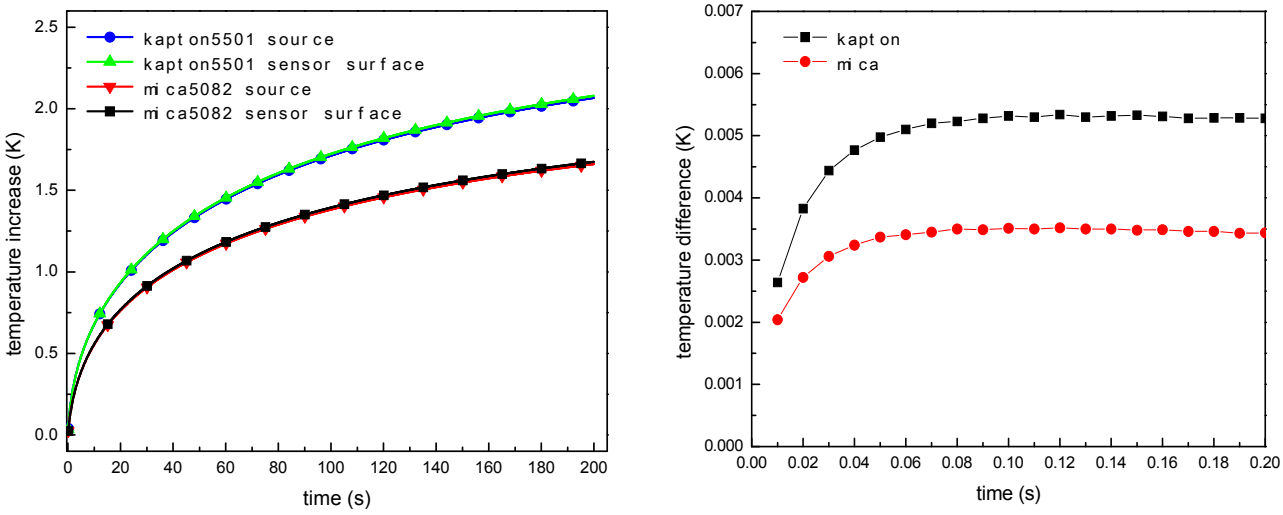

(a) (b)

4.4 The effect of heat loss through the sensor side on the thermal conductivity measuring accuracy

As shown in Table 7, the thermal conductivity deviation of silica aerogel measured by kapton5501 and mica5082 sensor reaches as much as 54.2% while the deviations of ceramic and stainless steel thermal conductivities measured by different sensors are only 2.86% and 1.92%, respectively. It indicates that the sensor material has great effect on the measurement of low thermal conductivity, such as the one of the silica aerogel. And actually, this finding in the authors' measurement practice motivated the present numerical study.

Table 7 Experiment and simulation comparisons of thermal conductivity

Material	*λ/W·m^{-1}·K^{-1}*	*Deviation/%*	*Sensor information*
Silica aerogel	0.03504	54.2	Experiment value of kapton5501
	0.05403		Experiment value of mica5082
	0.03200	-	Given value of simulation
	0.03291	2.84	Computational value of kapton5501
	0.04142	29.4	Computational value of mica5082
	0.03879	21.2	Computational value of mica4921
	0.03704	15.8	Computational value of mica4922
Ceramic	1.398	2.86	Experiment value of kapton5501
	1.438		Experiment value of mica5082
	1.450	-	Given value of simulation
	1.425	–1.72	Computational value of kapton5501
	1.416	–2.34	Computational value of mica5082
Stainless steel	13.52	1.92	Experiment value of kapton5501
	13.78		Experiment value of mica5082
	13.55	-	Given value of simulation
	13.27	–2.07	Computational value of kapton5501
	13.15	–2.95	Computational value of mica5082

Note: The experiments are conducted on the hot disk 2500S thermal constants analyser at room temperature.

Figure 7 Heat loss proportion through the sensor side, (a) stainless steel (b) ceramic and (c) silica aerogel (see online version for colours)

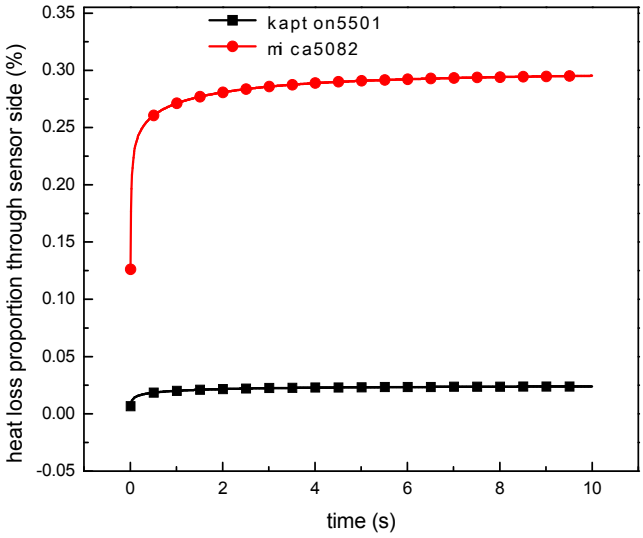

(a)

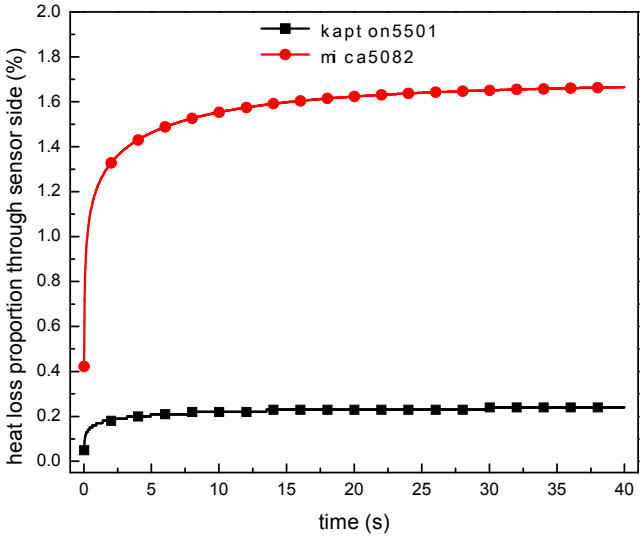

(b)

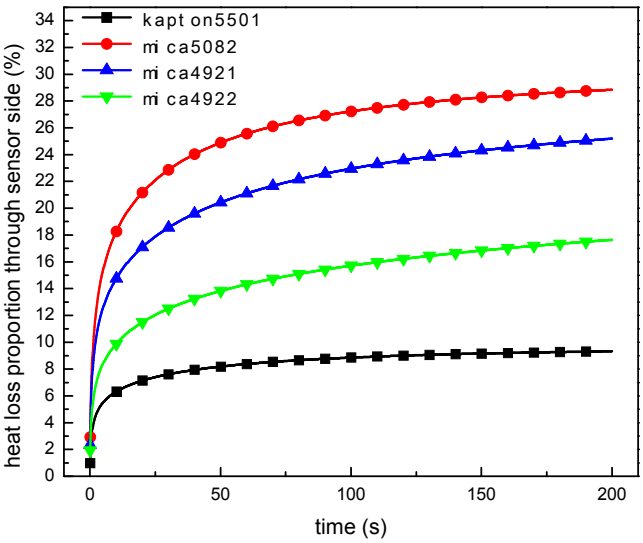

(c)

Figure 8 Heat loss proportion through the external boundary, (a) stainless steel (b) ceramic and (c) sillica aerogel (see online version for colours)

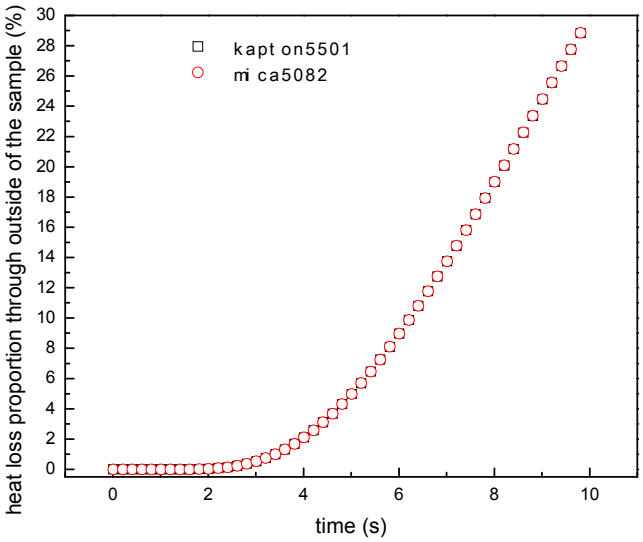

(a)

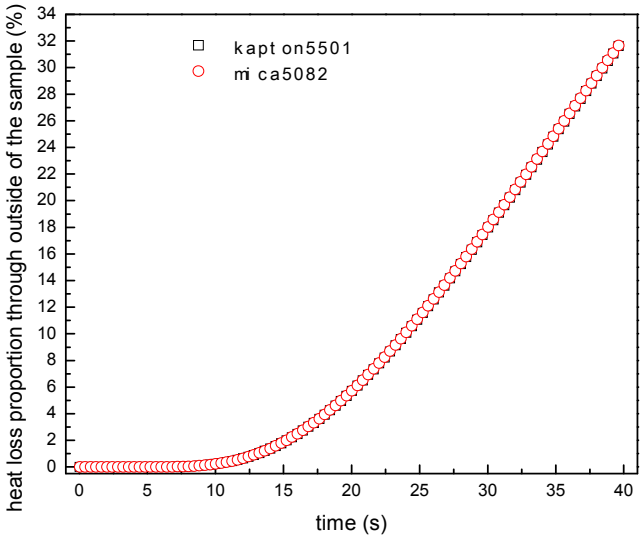

(b)

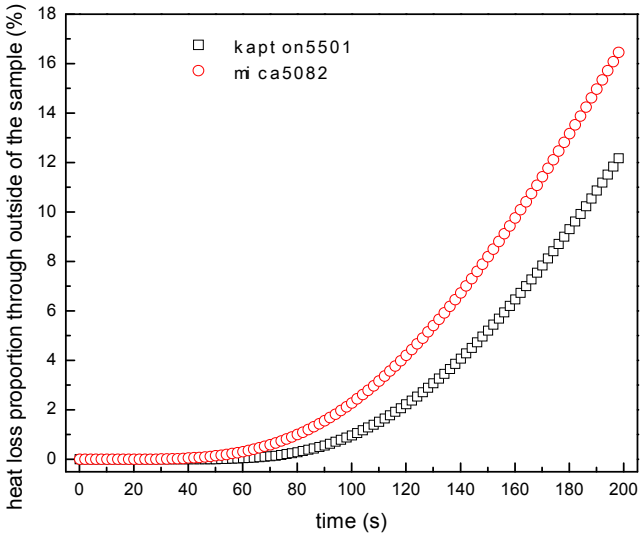

(c)

Numerical simulation of the real test process was conducted and the result is also shown in Table 7. During the simulation, the thermal conductivity of the material was given beforehand, and then the thermal conductivity could be calculated from the average temperature increase curve of the source. If the computational thermal conductivity value was very close to the given value, it proved that the sensor was suitable to measure that kind of material. The simulation result of stainless steel and ceramic shows that the deviations of kapton5501 sensor and mica5082 sensor are within ± 3% and agree well with the experiment result. The simulation result of silica aerogel also shows that the thermal conductivity values by using kapton and mica sensors are different.

The deviation between kapton5501 sensor and mica sensor decreases with the increases of the sensor radius. This is because the larger radius, the less heat loss through the sensor side. The heat loss proportion through different sensor side of different materials is shown in Figure 7. For the same material, the heat loss proportion through sensor side of mica is higher than that of kapton for its thicker insulation. For stainless steel and ceramic the proportion is less than 1.7%, therefore the deviation of different sensors is acceptable. However, for silica aerogel, the heat loss proportion reaches as high as 28% for mica5082 sensor and decreases significantly with the increases radius of sensor. In addition, the deviation will also be improved by reducing the thickness of the insulation layer.

4.5 Heat loss through the external boundary of the sample

The transient plane source method requires no heat loss from the outside circumference of the sample to fit the infinite model. Figure 8 shows the heat loss proportion through the external circumferential boundary of the sample of different materials. It can be seen that the heat loss through the outside of the sample is negligibly small at the beginning of the simulation process and the measurement should be conducted during this period, and then the proportion increases rapidly with time. For the sample with thickness of 15 mm and radius of 20 mm (25 for mica4921 and mica4922), the measurement time window of stainless steel, ceramic and silica aerogel should not exceed the critical time periods of 4.4 s, 16.8 s and 110 s (with maximum heat loss 3%), respectively. Otherwise, the relationship $R(t)$ with $D(\tau)$ will deviates from the ideal linear relationship after the critical time, deteriorating the accuracy of the measurement.

5 Conclusions

In this article, numerical simulation and experiment research are conducted to discuss several issues of the transient plane source method by using hot disk kapton5501 sensor, mica5082 sensor, mica4921 sensor and mica4922 sensor. The major findings are summarised as follows:

1 The programme developed in this work was successful to calculate thermal conductivity and thermal diffusivity once obtained the temperature increase curve of the heat source. The thermal conductivity and thermal diffusivity deviation between the experiment and the programmes was within ± 2.14% when calculated the same temperature increase curve that measured in the experiment.

2 Both the kapton5501 sensor and mica5082 sensor could measure the thermal conductivity of silica aerogel and stainless steel with high accuracy when the sensor has no thickness and without insulation layer in the simulation.

3 The influence time of the insulation layer lasts less than 100 ms for the insulation layer is thin and the power output is constant.

4 Both the kapton5501 sensor and the mica5082 sensor can be used for measuring materials with thermal conductivity larger than 1.45 W/m·K (ceramic) accurately because the heat loss proportion through the sensor side during the test process could be neglected. The numerical simulation proves that the large deviation of thermal conductivity when measuring silica aerogel with kapton5501 sensor and mica5082 sensor was caused by the large heat loss proportion through sensor side. The simulation found that the heat loss through sensor side decreases rapidly with the increases of the sensor radius.

5 The measurement time window of the transient plane source method should be neither too short nor too long to avoid the influence of the thermal resistance taking up large proportion of the measurement time and the heat loss through outside of the sample influencing the liner relationship between $R(t)$ and $D(\tau)$. The appropriate test time window for certain materials was obtained by experiment.

Acknowledgements

This work is supported by the National Natural Science Foundation of China (51136004) and the National Basic Research Programme of China (2010CB227102).

References

Bohac, V., Gustavsson, M.K., Kubicar, L. and Gustafsson, S.E. (2000) 'Parameter estimations for measurements of thermal transport properties with the hot disk thermal constants analyzer', *Review of Science Instruments*, Vol. 71, No. 6, pp.2452–2455.

Carslaw, H.S. and Jaeger, J.C. (1986) *Conduction of Heat in Solids*, pp.255–280, Clarendon Press, Oxford.

Cintra Jr., J.S. and dos Santos, W.N. (2000) 'Numerical analysis of sample dimension in hot wire thermal conductivity measurements', *Journal of the European Ceramic Society*, Vol. 20, No. 11, pp.1871–1875.

Gustafsson, S.E. (1990) 'Transient plane source techniques for thermal conductivity and thermal diffusivity measurements of solid materials', *Review of Scientific Instruments*, Vol. 62, No. 3, pp.797–804.

Gustafsson, S.E., Karawack, E. and Chohan, M.N. (1986) 'Thermal transport studies of electrically conducting materials using transient hot-strip technique', *Journal of Physics D-Applied Physics*, Vol. 19, No. 5, pp.727–735.

Gustafsson, S.E., Karawack, E. and Khan, M.N. (1979) 'Transient hot-strip method for simultaneously measuring thermal conductivity and thermal diffusivity of solids and fluids', *Journal of Physics D-Applied Physics*, Vol. 12, No. 9, pp.1411–1421

Hay, B., Filtz, J.R., Hameury, J. and Rongione, L. (2005) 'Uncertainty of thermal diffusivity measurements by laser flash method', *International Journal of Thermophysics*, Vol. 26, No. 6, pp.1883–1898.

Huang, L.H. and Liu, L.S. (2009) 'Simultaneous determination of thermal conductivity and thermal diffusivity of food and agricultural materials using a transient plane-source method', *Journal of Food Engineering*, Vol. 95, No. 4, pp.179–185.

ISO22007-2 (2008) 'Plastices – determination of thermal conductivity and thermal diffusivity-part 2: transient plane source (hot disc) method'.

ISO22007-4 (2008) 'Plastices – determination of thermal conductivity and thermal diffusivity-part 4: laser flash method'.

ISO8894-1 (1987) 'Refractory material – determination of thermal conductivity-part 1: hot-wire method (cross-array)', 1st ed.

ISO8894-2 (2007) 'Refractory material – determination of thermal conductivity-part 1: hot-wire method (parallel)'.

Malinarič, S. (2007) 'Uncertainty analysis of thermophysical property measurement of solids using dynamic methods', *International Journal of Thermophysics*, Vol. 28, No. 1, pp.20–32.

Saleh, A. and Al, A. (2006) 'Measurement of thermal properties of insulation materials by using transient plane source technique', *Applied Thermal Engineering*, Vol. 26, Nos. 17–18, pp.2184–2191.

Solorzano, E., Regero, J.A., Rodriguez-Pérez, M.A., Lehmhus, D., Wichmann, M. and de Saja, J.A. (2008) 'An experimental study on the thermal conductivity of aluminum foams by using the transient plane source method', *International Journal of Heat and Mass Transfer*, Vol. 51, Nos. 25–26, pp.6259–6267.

Suleiman, B.M. (2010) 'Alternative fitting procedures to enhance the performance of resistive sensors for thermal transient measurements', *Sensors and Actuators A*, Vol. 163, No. 2, pp.441–448.

Suleiman, B.M. and Malinarič, S. (2006) 'Transient techniques for measurements of thermal properties of solids: data evaluation within optimized time intervals', *WSEAS Transactions on Heat and Mass Transfer*, Vol. 12, No. 1, pp.801–807.

Suleiman, B.M. and Malinarič, S. (2007) 'Developments in the data evaluation of the EDPS technique to determine the thermal properties of solids', *WSEAS Transactions on Heat and Mass Transfer*, Vol. 4, No. 2, pp.99–110.

Xie, H.Q., Gu, H., Fujii, M. and Zhang, Z. (2006) 'Short hot wire technique for measuring thermal conductivity and thermal diffusivity of various materials', *Measurement Science and Technology*, Vol. 17, No. 1, pp.208–214.

Nomenclature

a	Thermal diffusivity of the test sample ($mm^2 \cdot s^{-1}$)
c	Specific heat ($J \cdot kg^{-1} \cdot K^{-1}$)
D	Dimensionless specific time function (–)
I	Modified Bessel function (–)
m	Number of concentric ring sources (–)
P	Power output of the sensor (W)
R	Electronic resistance of sensor (Ω)
r	Radius of the sensor (mm)
T	Temperature (K)
t	Time (s)
Greek symbols	
α	Temperature coefficient of the resistivity (K^{-1})
λ	Thermal conductivity of the test sample ($W \cdot m^{-1} \cdot K^{-1}$)
ρ	Density ($kg \cdot m^{-3}$)
τ	Dimensionless time (–)
Θ	Characteristic time (s)
Subscripts	
i	Represent the sensor insulation
p	Constant pressure